Long term trend in surface temperature in the Canary Islands from in-situ observations

Miguel Ángel Gutiérrez Guerra

Curso 2019-20

María Dolores Pérez Hernández

Pedro Vélez Belchí

Trabajo Fin de Título para la obtención del título en Grado en Ciencias del Mar

- ## Student data:

  Name: Miguel Ángel Gutiérrez Guerra

  Title: Grado en Ciencias del Mar

- ## Academic tutor data:

  Name: María Dolores Pérez Hernández

  Institution: Instituto de Oceanografía y Cambio Global (IOCAG)

- ## Cotutor data:

  Name: Pedro Vélez Belchí

  Institution: Instituto Español de Oceanografía (IEO)

Index

Abstract: Sea Surface Temperature (SST) data from remote sensing (AVHRR /NOAA) between 1999 and 2019 show a warming trend of 0.28ºC per decade in the oceanic waters of the Canary Currents Large Marine Ecosystem (CCLME) and a cooling of 0. 05ºC per decade in the strongest upwelling cells in the CCLME. However, there are only a few in-situ long term observations in the CCLME to validate these observed trends. Here we use a set of in-situ data provided by four buoys located between Gran Canaria and Tenerife islands from the "Puertos del Estado" network and surface data from the long-term observations program of the Spanish Oceanographic institute, RaProCan (Radial Profunda de Canarias), to validate de satellite observations in the oceanic and upwelling waters.The comparisons permitted to determine the uncertainty of the observed trends in the oceanic waters of the CCLME and, based on that, estimate the uncertainty in trends of the Eastern Boundary Upwelling System obtained from SST.

Keywords: Sea Surface Temperature, Upwelling, Remote Sensing, CCLME.

1. INTRODUCTION.

The Large Marine Ecosystems (LMEs) are a globalized approach to a management framework that defines and ranks marine regions based on their gross primary production (Sherman & Hempel, 2008). Many of the most productive LMEs of the world are linked to upwelling processes that supply nutrients and oxygen to maintain the high rate of primary production (Pauly & Christensen, 1995). This is the case of our study region, the Canary Current Large Marine Ecosystem (CCLME), named after the Canary Current. The CCLME is one of the four major Eastern Boundary Upwelling System (EBUS) in the world. Thanks to the nutrients that come from the upwelling, the CCMLE has on average a primary production of 1196 mgC m^{-2} d^{-1} which is about 8% of the primary production in the world ocean (Sherman & Hempel, 2008). The CCLME covers the latitude range 12-43º N and supports the fisheries of the surrounding countries like Spain, Portugal, Morocco, Mauritania, and Senegal (Kämpf & Chapman, 2016). Since the CCLME is an EBUS, it contributes to the development of the fisheries in the area and have a huge economic importance. Hence, this system was widely studied in the past decade (e.g. Pauly & Christensen, 1995)

The coastal upwelling in the CCMLE requires mainly three conditions: trade winds flowing parallel to the African and Iberian coast, the boundary conditions of the continental-self, and the influence of the Coriolis effects (Ekman, 1905). Those winds

cause offshore currents (known as Ekman transport) that transport surface water horizontally and perpendicular to the wind direction. Because seawater is largely incompressible, the same volume moving laterally is replaced by deeper water, which is cooler and richer in nutrients than the surface waters above (Kämpf & Chapman, 2016). This Ekman transport is not homogeneously distributed along the coast, changes in the orientation and depth of the continental shelf lead to the existence of more intense upwelling cells (Arístegui et al., 2009). Aristegui et al. (2009) described the seasonal upwelling regions in the Galician, Portuguese, and Mauritanian zone. The coastal upwelling vary seasonally following the latitudinal migrations of the atmospheric pressure system: in summer the Azores Highs affects the northern extreme (Galician and Portuguese subregion), and in winter it moves to the south, affecting the southern region (Mauritanian-Senegalese subregion) while in the center portion (Morocco subregion) upwelling lasts all year-round (Wooster et al., 1976).

The dynamics of the coastal upwelling in the LMEs have been altered due to the actual climate change scenario (Belkin, 2009). Bakun (1990) hypothesized that the actual climate change scenario could lead to an intensification of the coast-ocean temperature gradient due to the inhibition of the night-time cooling and a build-up of the daytime heating. This heat difference would reinforce the wind curl stress and, therefore, cause an increment of the upwelling intensity (Bakun, 1990). Several authors studied the trends of several variables related to the upwelling like wind stress or Sea Surface Temperature (SST) to prove this hypothesis (Barton et al., 2013; Belkin, 2009; McGregor et al., 2007; Narayan et al., 2010). When considered global studies, this hypothesis is often rejected in the bibliography except for the Humboldt and California current systems where a cooler trend was detected (e.g. Belkin, 2009). Regional studies in the CCMLE like McGregor et al. (2007), found strong support for Bakun's hypothesis in the Cape Ghir area. McGregor et al. (2007) study is based on SST proxies derived from two sediment cores using an alkenone unsaturation index ($U_{37}^{K\prime}$) extracted from coccolithophorids. They concluded that the SST of the upwelling varies in opposite direction to the millennial timescale changes the Northern Hemisphere temperature anomalies (NHTAs). This means that, like propose by Bakun (1990), warming of the water results in cooler signals of SST in upwelling regions (McGregor et al., 2007). Also, supportive results for Bakun's hypothesis were found with an upwelling index based on the difference of SST offshore and at the coast (Narayan et al., 2010). However, more recent work from Barton et al, (2013) discusses the proxies derived from the $U_{37}^{K\prime}$ of McGregor et al (2007) and argued that lower SST signal detected in the $U_{37}^{K\prime}$ may be explained by the deepen of the coccolithophorids distribution in the water column. The discussion about the changes in the upwelling areas under global warming remains open and with abundant uncertainties.

A few physical variables such as SST or wind stress are key in the forecast of this important process.

SST is an important variable to better understand the climate system and therefore there is a wide variety of applications in fields such as fisheries or coastal management (Eugenio et al., 2005). In the study of EBUS, we can detect the coastal upwelling from the SST because, (as described before) upwelling transports deep cool water masses into the surface, imprinting a cool signature over the warm subtropical ocean. It is generally recognized that reliable measures of SST data began in 1850 from thermometers in a bucket of seawater (Rayner et al., 2006). Around 1970, motivated by the operational requirements for weather prediction and navigation safety, the USA and other countries installed moored buoys generally around the coast (Woodruff et al., 2008). At the same time, the first Infrared satellite (IR) started to collect data. IR scanning radiometers on geostationary orbit took images of the earth's disk, even in the 1970s. These images were frequently provided to increase the chances of observing cloud free ocean sections (Legeckis, 1975).

Satellite data provide both high spatial and temporal sampling resolution. However, it often suffers atmospheric interruptions due to water vapor or volcanic eruptions that lower the quality of the observational time series (Minnett et al., 2019). Therefore, the *in-situ* observations are a keystone in the validation of the satellite data. It was not until the first launch of the AVHRR (The Advanced Very High-Resolution Radiometer) from the NOAA (National Oceanic and Atmospheric Administration), on the TIROS-N satellite in 1978 (Cracknell, 1996), that SSTs were not routinely produced. Initial validation of the AVHRR SSTs consisted of an atmospheric correction algorithm that produced a standard deviation with differences depending on the source of the validating record (McClain et al., 1985). In the development of the SST remote sensing, the Group of High-Resolution SST (GHRSST) played a key role as an international platform to discuss and compare results. However, the most important step was to produce an international framework to recollect and store remote sensing SST data (Minnett et al., 2019). This included an uncertainty estimation by considering all the likely sources of error like cloud contamination, or coastal interference for the infrared or rainfall in the case of the microwave (Donlon et al, 2007). Also, GHRSST provided with useful products like the GMPE (GHRSST multi-product ensemble) that combined several datasets with complementary features such as: the AVHRR data with good global high-resolution coverage and the AMSR-E (The Advanced Microwave Scanning Radiometer) which thanks to the use of microwave it worked even in cloud presence. Finally, the in-situ observations corrected the bias in the satellite sets (Donlon et al., 2012). As the satellite sensors improved, along with the algorithm corrections, the difference between *in-situ* SST and SST-derived became smaller so the error contributions of the interference were

no longer of second order and could not be ignored (Minnett et al, 2019). So, the importance of the in-situ data and their control gained weight.

Nowadays, *in-situ* data are available from many platforms divided into vessel-based observations, drifting platforms, and moored buoys, each with different performances. The drifting buoys are the most used for their large geographical coverage and availability in near real-time thanks to the Global Telecommunication System (Minnett et al, 2019). On the other hand, moored buoys provided long- term consistent measurements of a single area and allow us to control the stability of the satellite records (Merchant et al., 2012). The Vessel-based observations provides measurements in the whole water column with an intermedium range of geographical. However, the measured frequency is usually lower than the moored buoys.

In this work, we will estimate the uncertainty of the trends in SST-derived satellite with several *in-situ* datasets and elaborate a method to correct the SST observed from satellite. We also evaluate the trends in the region of CCMLE from corrected SST-derived satellite. Overall, the objective of this study is to assert the validity of the observed satellite trends in the SST and determine if there is a significant difference between the trend in the oceanic and upwelling waters, that would indicate the validity of the Bakun's hypothesis in the CCLME. This work is structure in 6 sections: section 2 will expose the diverse datasets used, section 3 will detail the methods used in this work, section 4 will present the results obtained through the analyses made, in section 5 results will be discuss and compare with others studies and section 6 will resume the conclusions of this study, finally all the references used in this work will present in section 7.

2. DATA.

This study aims to validate satellite SST data from the most common databases with *in situ* observations from moored buoys, provided by 'Puertos del Estado'. The *in-situ* SST data sets were selected in the Canary Island in the 1996-2019 time period (table 1), and the SST-derived satellite records from 1982 to 2019. Positions of *in-situ* data shown in figure 1 and more details of every data sets are found in table 1. Satellite products locations were chosen to match *in-situ* observations for statistical analysis, by finding the closest point in the satellite grid to the *in-situ* data (figure 1, open circles). The complete satellite data set was used for regional analysis.

Table 1. Satellite data. Geographical region and time period covered.

Data Base	Source	Latitude	Period
AVHRR/NOAA	https://www.esrl.noaa.gov/psd/data/gridded/data.noaa.oisst.v2.highres.html	11.5-45º	1982-20
GHRSST	https://opendap.jpl.nasa.gov/opendap/allData/ghrsst/data/GDS2/L4/GLOB/JPL/MUR/v4.1/	11.5-45º	1982-20
MODIS	https://oceandata.sci.gsfc.nasa.gov	11.5-45º	2002-20

The primary satellite source of SST used here is the new AVHRR/NOAA reanalysis (Reynolds et al., 2007). This data set improved by using Optimum Interpolation (OI) techniques and downscaled the spatial resolution from 1º to 0.25º regular grid and a temporal resolution of 1 day. This data set also introduced the AMRS sensor which combined with the AVHRR provide an almost all-weather data. The reanalysis uses in-situ data for a larger-scale adjustment of the satellite biases.

The GHRSST product provides a grid with a spatial resolution of 1 km and a temporal resolution of 1 day and measure SST and sub skin SST from different instrument including the used in the NOAA product and others such as the JAXA Advanced Microwave Scanning Radiometer 2 on GCOM-W1 satellite, the Moderate Resolution Imaging Spectroradiometers (MODIS) on the NASA Aqua and Terra platforms, the US Navy microwave WindSat radiometer. Also, it includes *in-situ* measures from the NOAA iQuam project.

The MODIS satellite data set, from NASA is the last of the satellite products used. It has a moderate spatial resolution of 1º grid and temporal resolution of 1 week. Unlike the others is not a reanalysis product so it only uses correction algorithms to adjust the biases of the data.

Table 2. *In-situ* data. Geographical region and time period covered datasets. EN4, the RaProCan survey (second row), the REDEXT buoys (third and fourth row) and REDCOS buoys (last rows).

Data Base	Source	Latitude	Period
EN4	https://www.metoffice.gov.uk/hadobs/en4/download-en4-2-1.html	11.5-45ºN	1982-20
RaProCan	https://www.oceanografia.es/raprocan	28.5-29ºN	1996-19
GC	www.puertos.es/es-es/oceanografia/Paginas/portus.aspx	28.2ºN	2001-19
TS	www.puertos.es/es-es/oceanografia/Paginas/portus.aspx	27.99ºN	2001-19
SC	www.puertos.es/es-es/oceanografia/Paginas/portus.aspx	28.46ºN	2009-19
PE	www.puertos.es/es-es/oceanografia/Paginas/portus.aspx	28.05ºN	2014-20

Moored buoys from "Puertos del Estado" in the Canary Islands provide consistent long-term series with hourly intervals. Specifically, we will use data from four buoys located in the vicinity of Gran Canaria and Tenerife with almost twenty years of data. There are two different projects maintaining this dataset with different features: the REDEXT and the REDCOS (table 2). REDEXT places Seawater buoys in deep waters (around 740 m) that measure SST at 3 m. These measurements area available since 2003 (table 1). Two buoys belong to this project, named hereafter as "Tenerife Sur" (TS) and "Gran Canaria" (GC) as they are in the south of Tenerife and in the northwest side of Gran Canaria, respectively. In shallow waters, the REDCOS project started to record data usually near a harbor (depth less than 100m). It measures data mainly for wave analysis but some of their buoys like "Santa Cruz" (SC) and "Las Palmas Este" (PE) also collect oceanographic variables like SST. Those data are influenced by the bottom and the action of waves. These buoys did not start simultaneously their measurements. "Santa Cruz de Tenerife" started in 2009 while the buoy of "Las Palmas Este" began in 2014 (Table 2).

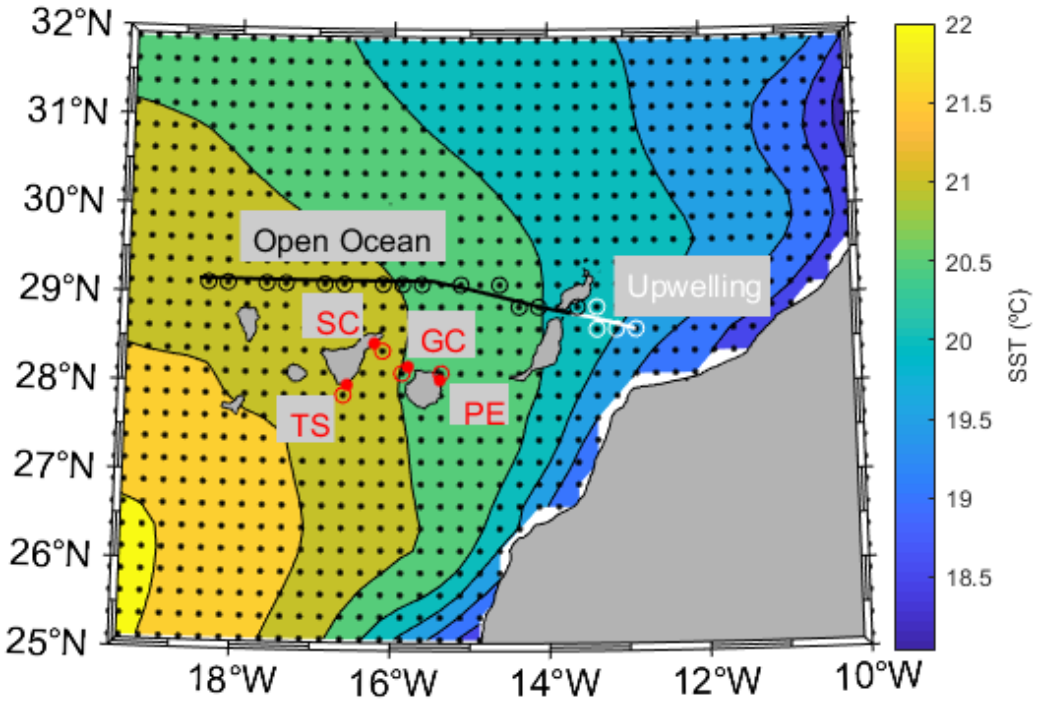

Figure 1: Position of the *in-situ* datasets used in this study: satellite-derived SSTs (black dots), "Puertos del Estado" Buoys (red dots) and the RaProCan survey (black and white lines). Open circles denote, in their respective colors, the closest point of the satellite grid to the observations. The Background field shows the average SST. In this study the results are divided into the upwelling zone (white) and the Open ocean zone (black).

A product commonly used, the EN4 dataset from the Met Office Hadley Center, has been used in the comparison with in-situ and satellite observations. This is the fourth version of a dataset that collects global observations from diverse sources like Argo floats or the World Ocean Database (WOD09), and interpolates them into a monthly product with a spatial resolution of 1º-degree gridded (Good et al., 2013). Although this product offers monthly data from 1900 to the present, it improves greatly with the onset of the Argo program (around 2005). Though data from 1900 to the present are available, only data since 1982 to 2020 were extracted. The EN4 dataset does not assimilate either the data from the other in-situ data used in this study, therefore the comparison between EN4 and other datasets may be made.

These observations are complemented with data from the Radial Profunda de Canarias (RaProCan) hydrographic section (Pedro Vélez-Belchí et al., 2017). RaProCan is the longest hydrographic times series in the eastern subtropical Atlantic and consists of 24 hydrographic stations around the Canary Island in which oceanographic variables like temperature, salinity, oxygen, etc... are measured in the full water column. In this work, we will only use the surface measurements of the 24 stations that expand along the northern side of the Canary Islands and reach the northwest coast of Africa through the

passage between Fuerteventura and Lanzarote. This cruise aims to establish the scale of variability in the range decadal in the North Atlantic subtropical gyre (Vélez-Belchí et al., 2014). To serve the purpose of our study the transect was divided into two subsections: one representative of the open ocean starting west of Lanzarote, and the other as a proxy of the coastal upwelling from Lanzarote to the east. The objective of this division is to better-calibrate the satellite observations in each one of these different dynamics, environments.

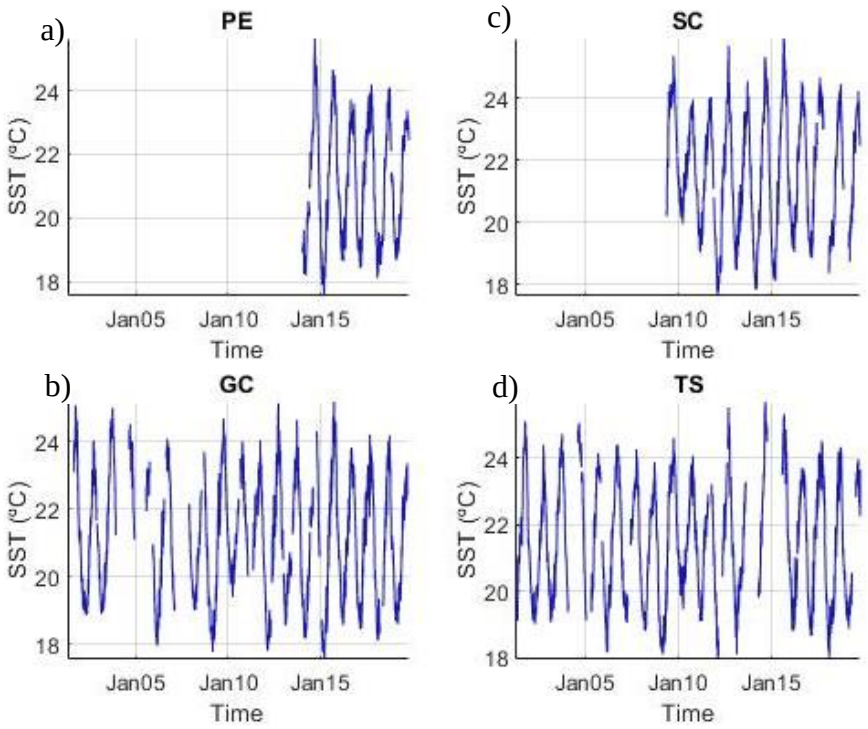

Figure 2: Daily average timeseries from the buoys of "Puertos del Estado". Las Palmas Este and Santa Cruz (a and c) that belong to the REDCOS project. And b) and d) are from the REDEXT project, called Gran Canaria and Tenerife Sur, respectively.

3. METHOD

Climate is a complicated process that involves several systems, mainly the atmosphere and the hydrosphere but also the biosphere, cryosphere, and lithosphere. Therefore, climate trends require a careful statistical analysis (Mudelsee, 2019). As a part of the pre-analysis, to reduce the daily noise we calculated the daily averages of the hourly data from buoys (figure 3b). Then, since we are interested in the long-term trends and not in the seasonal amplitude**,** we deseasonalized the data by estimating an annual average climatology (figure 3a, red line), This annual cycle contained the mean SST for each day of the year (Figure 3a, black dots), and therefore reflects the average seasonal cycle. Once the seasonal cycle is obtained, it is subtracted at each corresponding day from the time series, resulting in a deseasonalized time series (figure 3c). Another benefit of the use of the deseasonalized series is that the seasonal cycle is a common signal between the satellite and in-situ data and increase the correlation between them. In the case of the RaProCan dataset, the temporal resolution of the RaProCan dataset does not allow the estimation of the year-average climatology, hence, we use the satellite closest point in the grid to the RaProCan (figure 1) to deseasonalized the data set.

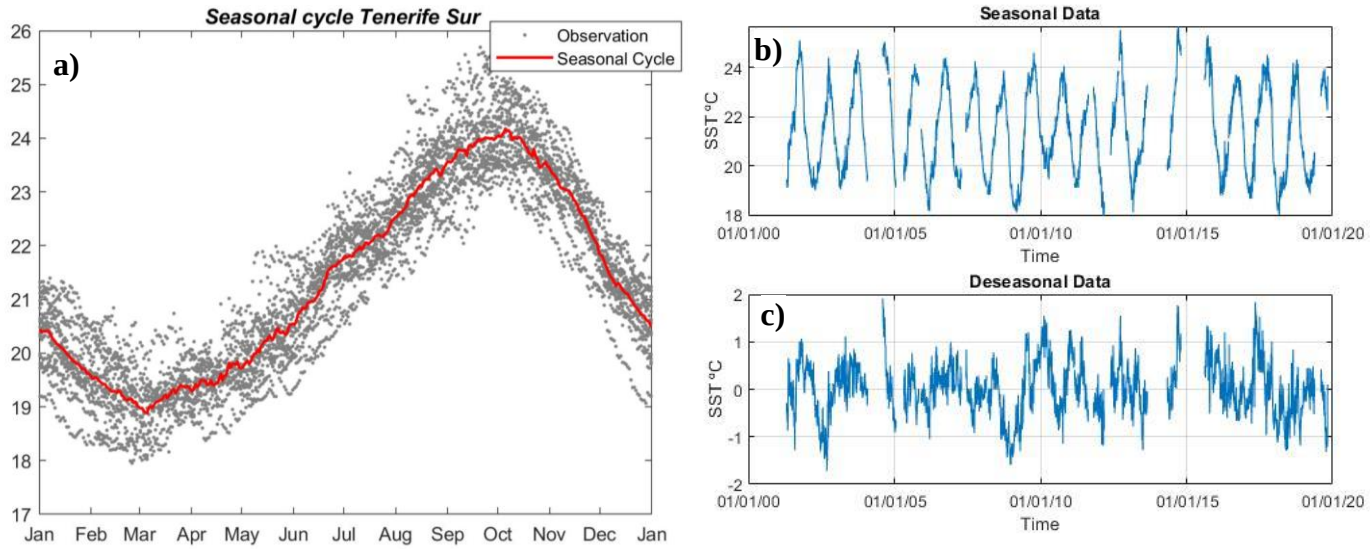

Figure 3. Example of the deseasonalizing process for the buoy of Tenerife Sur. First, we calculated the annual average (red line) from all the observations of the buoy (grey dots). In (b) we see the daily data with a strong seasonal cycle while (c) shows the data after eliminated the seasonal cycle (a) to the data (b)

The trends components in the time-series were calculated from the statistical model called linear regression. It describes the trends as a simple equation with two parameters: the slope (β_1) and the interception (β_0).

$$Y_t = \beta_0 + \beta_1 * t \qquad \text{eq (1)}$$

For the estimation of the coefficients (β_0, β_1) there are several methods available. In this work we use ordinary least square method (OLS).

The OLS minimizes the sum of the square differences between the data and the linear fit.

$$SSQ(\beta_0, \beta_1) = \sum x - \beta_0 - \beta_1 * t \qquad \text{eq (2)}$$

To find the minimum of this equation, its derived is set to zero. Finally, this gives us two equations with analytical solutions, this method arrived at estimators of the coefficients so received the notation $(\widehat{\beta_0}, \widehat{\beta_1})$ (Mudelsee, 2019). eq (3)

$$\hat{\beta}_0 = [\sum x(i) - \widehat{\beta_1} * \sum t]/n$$

$$\hat{\beta}_1 = \left\{[\sum t(i)] * \left[\frac{\sum x(i)}{n}\right] - \sum t(i) * x(i)\right\} * \left\{\frac{[\sum t(i)]^2}{n} - \sum [t(i)]^2\right\} \quad \text{eq (4)}$$

The coefficients of the regression line are also estimated by robust methods that are less sensitive than OLS to outliers (Alma, 2011)If great divergences between the robust methods and the OLS were found could reveal us the presence of outliers. The robust methods work out by weighed each point of the data through a weight function (w(r)). On the contrary that with the OLS solution, here we come to a set of nonlinear equations. The solution required a numerical method, we used the iteratively reweighted least square (IRLS). The IRLS problem could be expressed as the following matrix problem:

$$X'WX\hat{\beta} = X'W \quad \text{eq (5)}$$

Where W is an n x n diagonal matrix of weights, by default the MathWorks'® function *robustfit* update W in each iteration following the called biweight function (Beaton & Tukey, 1974):

$$w(r) = (1 - r^2)^2. \text{ For } |r|<1. \quad \text{eq (6)}$$

$$0 \qquad \text{Else.}$$

The variable r represents normalized residuals of the model and, logically, are updated after each iteration.

Initial parameters of the estimate coefficients vector, $\hat{\beta}(\hat{\beta}_0, \hat{\beta}_1)$, are set with the OLS method and update in each iteration (Alma, 2011):

$$\hat{\beta} = (X'WX)^{-1}X'W. \quad \text{eq (7).}$$

4. RESULTS

4.1. Puertos del Estado Network

The trends from the monthly deseasonalized SST for each one of the "Puertos del Estado" buoys used show similar behavior. As expected by its proximity, all have similar negative trends, although the PE and SC buoys present higher negative trends than the other buoys. However, these two buoys have a shorter time series, than was sampled during a pronounce decrease on the SST. This SST drop may also be seen in the final five years of the GC buoy (In almost the same period that the PE buoy). In the case of the TS and SC buoys, a smoother drop is detected. The two regression methods used do not divergence significative. As we said in section 3, because the robust method is less sensitive to anomaly values, convergence between both methods (OLS and IRLS) indicated the presence of outlier unlikely.

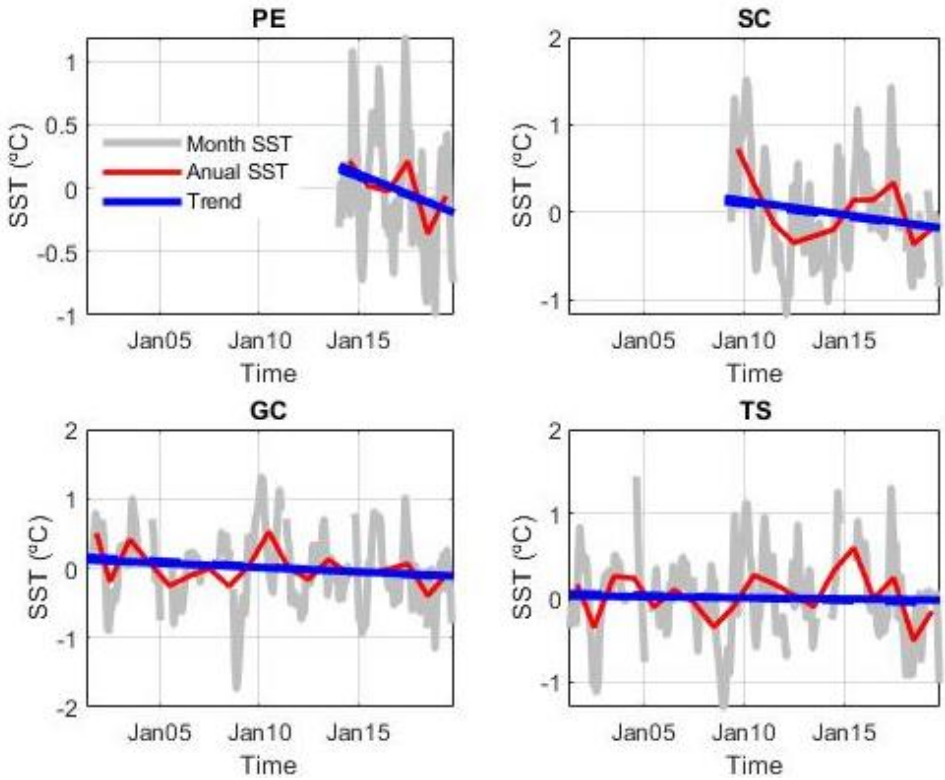

Figure 4: Trends calculated for all the "Puertos del Estado" Network. The grey line represents the monthly SST average, the red line the annual average and finally the blue line represent the ordinary trend while the blue dashed line shows the robust trend.

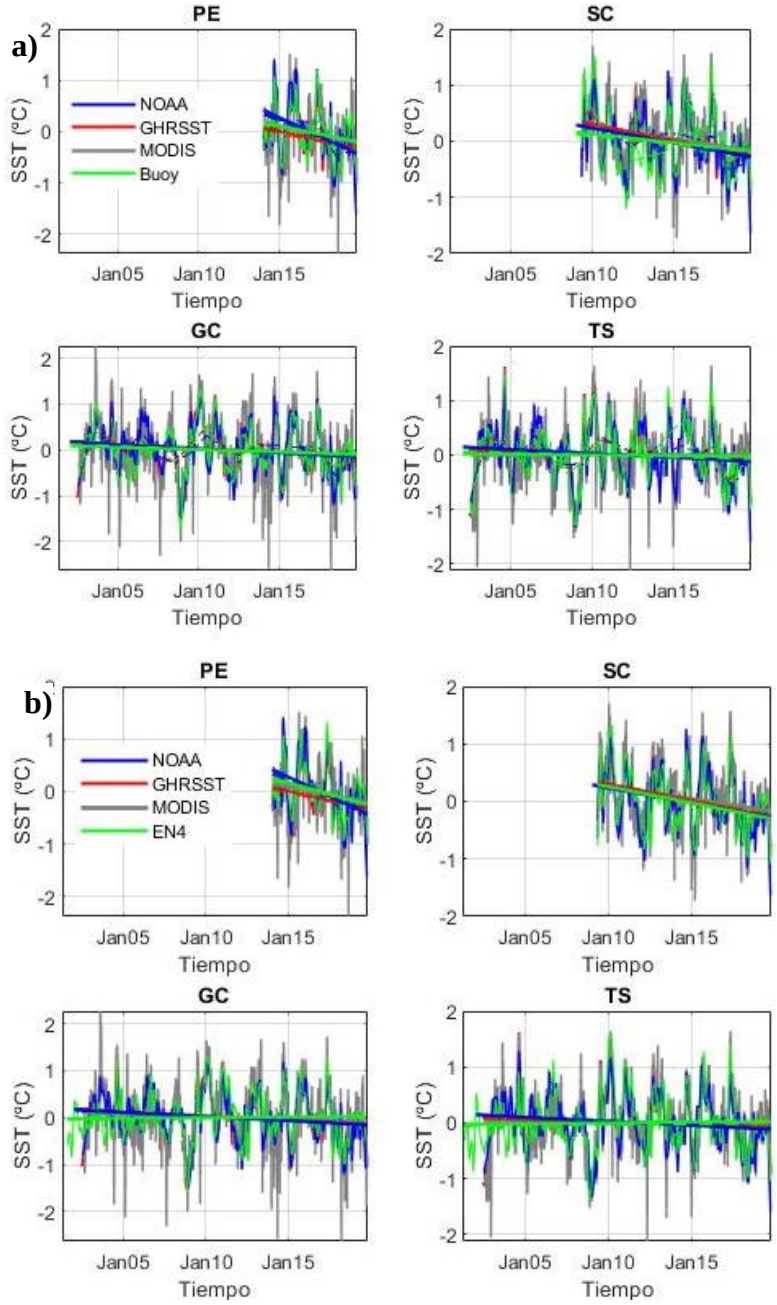

Figure 5: Comparison between different datasets. Each color represents a dataset as show by the legend. The straight line is the OLS trend. Different *in-situ* datasets are used: **a)** present the comparison between satellite and Puertos del Estado buoys and **b)** using the EN4 product as *in-situ* data.

There is good agreement between the remote sensing and the *in-situ* records as show in figure 5. In figure 5a, the comparison with all the satellite datasets at the location of each buoy is made to select the satellite product with greater likeness to the *in-situ* observations. Since all the datasets have similar trends (table 3), from now on, we will only use the AVHRR /NOAA satellite product from as representative of all the remote sensing records. Additionally, is the one most extensively used in the bibliography. The remote sensing data is more correlated with the buoys than with the EN4. The EN4 series

show high differences with the rest of the datasets until approximately 2005 (figure 5b). In this work we are especially interested in long-term analysis. So, the agreements between the trends of the different products is important.

Table 3. Trends and uncertainty (ºC/Decade) for each of the buoys (first row), and at each buoy location (see Figure 1 open circles) estimated from the EN4 (second row) and satellite datasets (last rows). Bolded trends represent those statistically significative.

Datasets	**S.C.**	**P.E.**	**T.S.**	**G.C**
"Puertos del Estado"	-0.010±0.011	-0.021±0.021	-0.0008±0.004	-0.004±0.005
EN4	**-0.018±0.009**	**-0.029±0.021**	0.001±0.004	0.0009±0.004
GHRSST	**-0.019±0.008**	**-0.023±0.022**	-0.002±0.004	**-0.006±0.004**
MODIS	**-0.015±0.005**	**-0.021±0.026**	0.0002±0.002	**-0.005±0.003**
AVHRR/NOAA	**-0.017±0.009**	**-0.048±0.025**	-0.003±0.004	**-0.005±0.004**

The confident intervals (collected in table 3) show us which trends are statistically significative (those that not include the 0 in their intervals), and therefore values bolded in table 3 indicates the trends which their uncertainty allow us to determinate, in a statistical way, its significative. Additionally, all the trends are superimposed if we considered the confident intervals at 95%, which imply that the underlying signal is coherent between all the above data sets.

4.2. RaProCan

For the RaProCan time series, we created two subsections as we mentioned in section 2. In the subsection used as proxy for the upwelling area the trends of *in-situ* data and satellite are opposite as show in figure 7, and any of them is statistically different from zero. As we expected the remote sensing becomes gradually sensible as the measurement approximates to the coast.

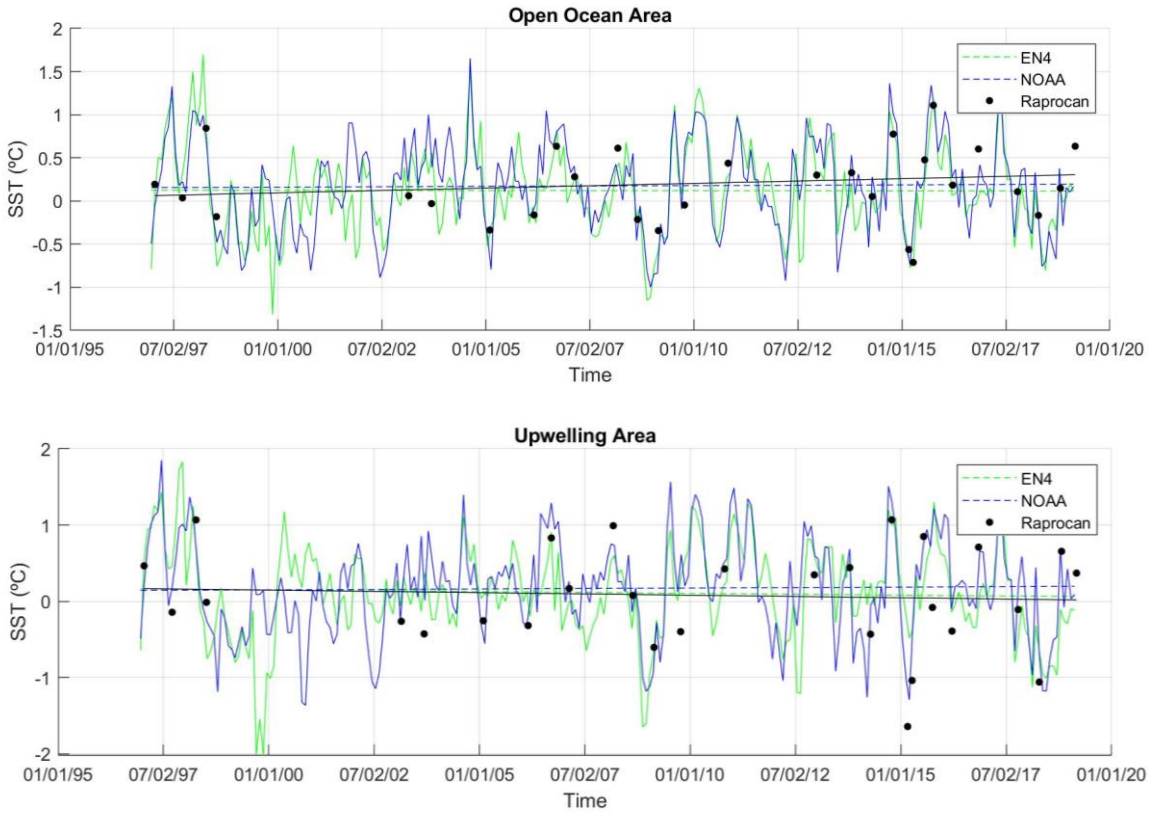

Figure 6: Deseasonal data and their trends are presented for the two subsections of RaProCan. The Open Ocean zone northern of Canary Islands (upper panel) and the Upwelling area (lower panel) as a proxy of the Upwelling off the Morocco coast. Blue line represents the data of the NOAA product and the dashed line show its trends. The green color represents the EN4 data with the same scheme (solid line for the data and dashed for the trend). Finally, black dots show the measures of RaProCan survey and black solid line show the trend.

In table 4 we include the trends computed for the RaProCan timeseries. Though the *in-situ* trends of the subsections diverge, they present large confident intervals due to the limited length of data available for this project, and therefore there is a larger uncertainty. However, the satellite derived-SST have similar trends in both areas.

Table 4. Trends and uncertainty (ºC/Decade) for the RaProCan area from the hydrographic cruise (first row), EN4 product (second row), and AVHRR/NOAA satellite data (last row)

Datasets	**Open Ocean Area**	**Upwelling Area**
RaProCan	0.007±0.017	-0.004 ± 0.025
EN4	-0.0001± 0.006	-0.003 ± 0.007
AVHRR/NOAA	0.001± 0.006	0.002 ± 0.008

The EN4 shows again discrepancy with the rest of datasets. Also, in this area disagreements seem to hold on until approximately 2005. From 2005, the EN4 record though it presented little disagreements, reflects the variability of the data. For all the datasets the confident intervals (and therefore the uncertainty) become larger in the proxy to the Upwelling. The confident intervals depend on the residuals of the models and the length of the data. A larger interval implies a more disperse residuals and in the case of the RaProCan data this effect is intensified by the lack of data.

4.3. Transference Function.

Taking advantage of the *in-situ* observations in the area, we will determine the correlation between *in-situ* and satellite data to elaborate a transfer function that calibrate the satellite data. The correlation is calculated through ordinary regression between the series, the slope of the regression indicates the correlation. The nearer to a slope coefficient of 1 the better will be the correlation. Regressions were calculated for both Open Ocean zone and the quasi-Upwelling Area. The Open Ocean used the average data of all the buoys from "Puertos del Estado" instead of the RaProCan survey, as the "Puertos del Estado" dataset is longer. But in the Upwelling zone the resources are limited and the only available record is the data from the RaProCan surveys since the EN4 data are not totally reliable, due to the lack of in situ observations to assimilate, as demonstrated previously.

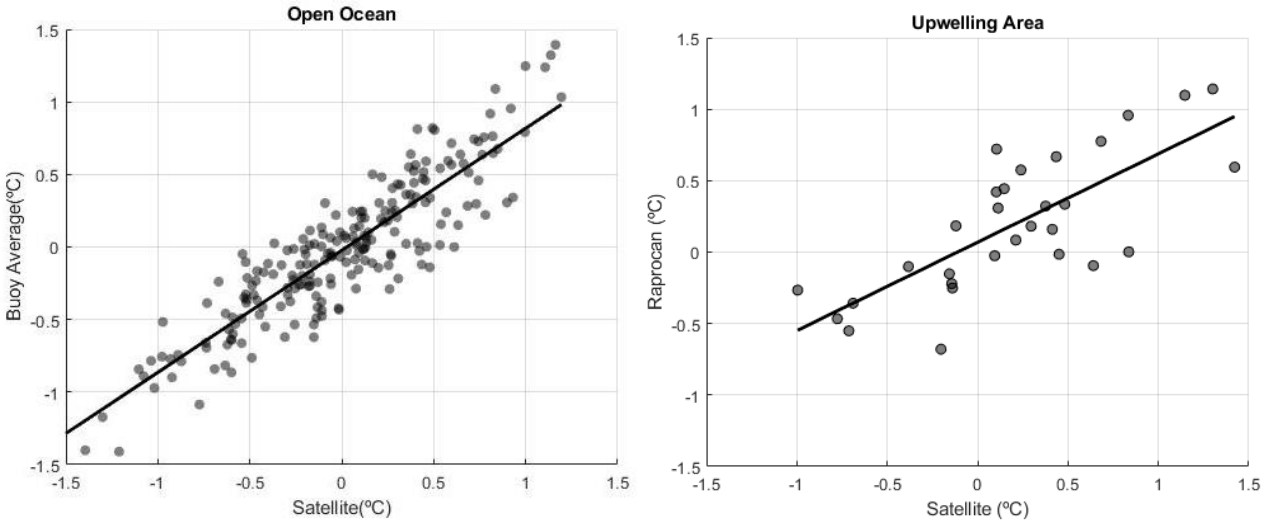

Figure 7: Regression between *in-situ* and remote sensing data. On the left, the regression of the open ocean area and on the right, the regression of the proxy for the upwelling area.

From the OLS we obtained an equation for each area:

For the Open Ocean Area:

$$Y_{Insitu} = 0.8412^{*} X_{Sat} - 0.0231 \qquad \text{eq (8)}$$

For the Upwelling Area:

$$Y_{Insitu} = 0.6186^{*} X_{Sat} + 0.0691 \qquad \text{eq (9).}$$

The slope is closest to 1 in the open ocean area, as expected. As this parameter was an estimation through the OLS method as the trend it has an uncertainty associated. Thus, confident intervals: In the case of the open ocean region the interval is ±0.02917, and for the upwelling area the confident interval estimate is ±0.0994. Both are statistically significative but more important although, the uncertainty growth, the slope coefficients of both areas do not match. The inferior limit of the slope in eq (8*)* is 0.812 and the upper limit of the eq (9) is 0.718.

But there are other important parameters we may extract from the regression. The R^2 predicts how good the regression fit the data, in other words, it is an index of the validity of the regression. As nearest to 1 the better will be the fit. For the open ocean zone, the R^2 is 0.719 an acceptable value for experimental data. In the case of the Upwelling area the R^2 is lower, 0.565, as there is a lack of data.

4.4. The CCLME.

We apply eq (8 and 9) to correct the satellite data from the AVHRR/NOAA in the whole CCMLE region (figure 9). We have identified the Open Ocean or the Upwelling areas to apply the transfer functions based on the surface gradient.

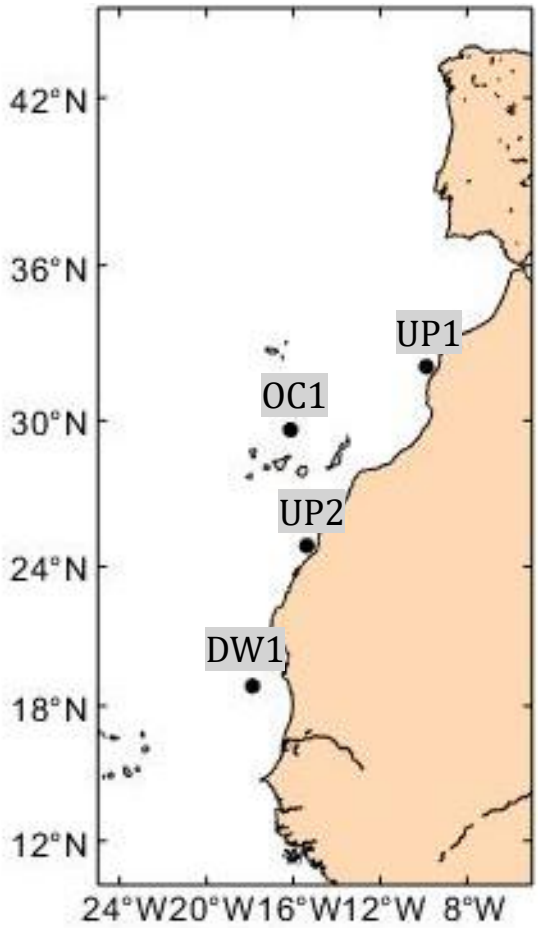

Figure 8: Map of the CCLME with the coordinates of the four series selected for exemplified the corrections of the satellite grid.

To study the long-term changes in the CCLME we have selected two upwelling cells (UP1 and UP2), and two coordinates representative of the open ocean behavior (OC1) and the downwelling cell (DW1). UP1 and UP2 represent the upwelling cells of cape Ghir and the Morocco subregions, respectively, described by Arístegui et al, 2009. OC1 is close to the Canary island, near to the *in-situ* observations used in the previous analysis of RaProCan.

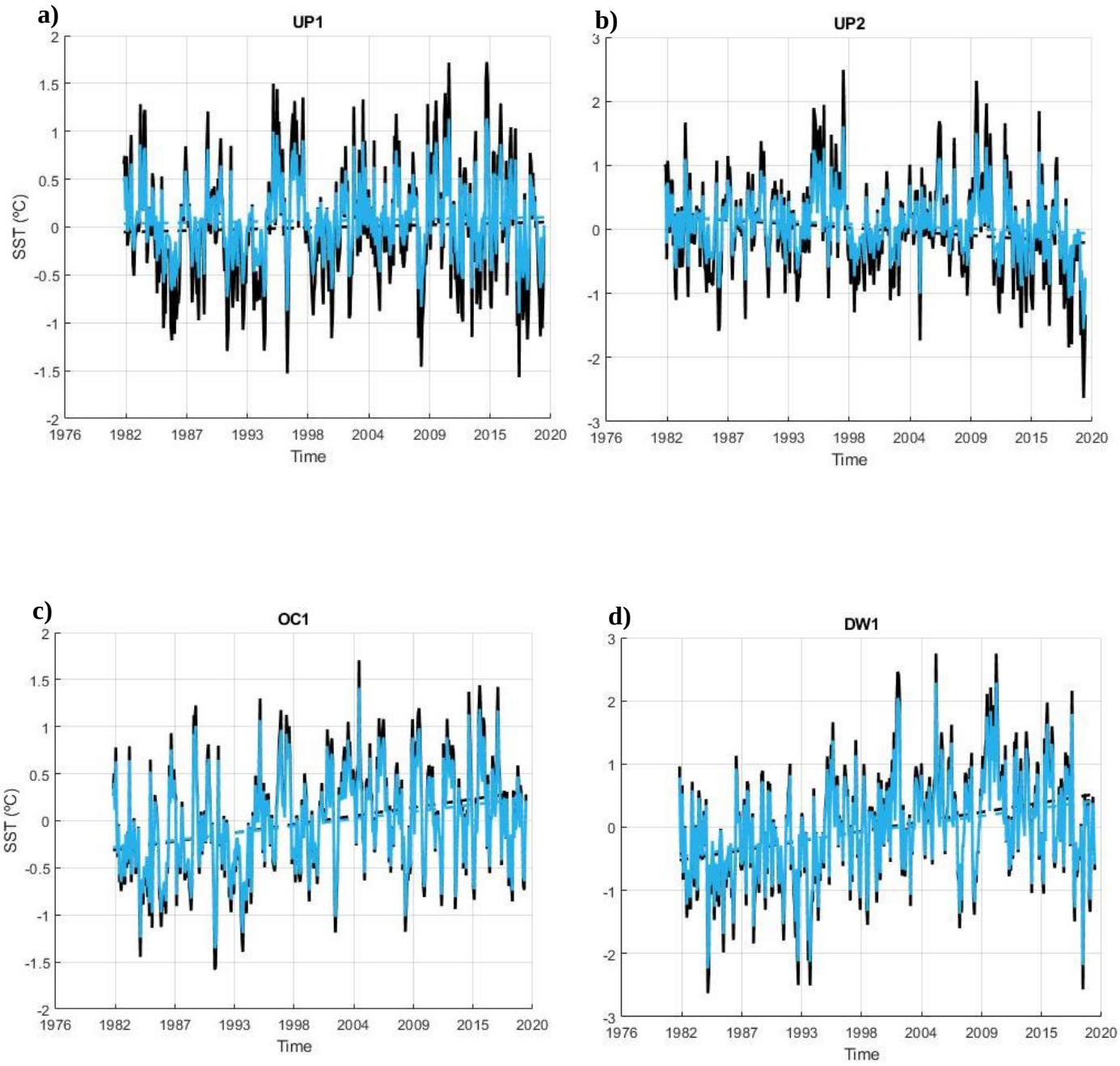

Figure 9: Show the corrections made by the transference functions. Black line is not corrected series and the blue lines the same series after the application of the transference function, the dashed lines of each color are their trends. **a)** and **b)** represent the series of UP1 and UP2, respectively. **c)** and **d)** correspond to the OC1 and DW1 coordinates.

As the figure 10 show, the calibration reduces the variability of the series in all the cases. But the upwelling area suffer a lower reduction due to the weaker correlation shown in section 4.2. This also reduce the trends (table 5), however the sign of the trend does not change.

Table 5. Trends and uncertainty (ºC/Decade) of the CCMLE regions selected for study the corrections.

Datasets	Uncorrected	Corrected
UP1	0.027 ± 0.051	0.017 ± 0.032
UP2	**-0.110 ± 0.061**	**-0.068 ± 0.038**
OC1	**0.164 ± 0.046**	**0.138 ±0.039**
DW1	**0.276 ± 0.070**	**0.232 ± 0.059**

The upwelling associated to UP1, at Cape Ghir, is not permanent. This is reflected in its trend which is the only one non statistically significative of the four selected. The UP2, corresponds to the permanent Morocco upwelling cell and shows a negative trend even after the corrections. This negative trend suggests an intensification of the permanent upwelling centers existing along the African shelf. In the open ocean zone, the trends are significantly positive, and larger for the downwelling cells. Probably because a similar intensification of the process.

The corrections were applied to all the satellite data of SST data from the CCMLE (figure 11). Several negative trends areas are detected along the African coast, and one strongly positive trend center around 18ºN. These centers suggest an intensification of both processes upwelling and downwelling in the region

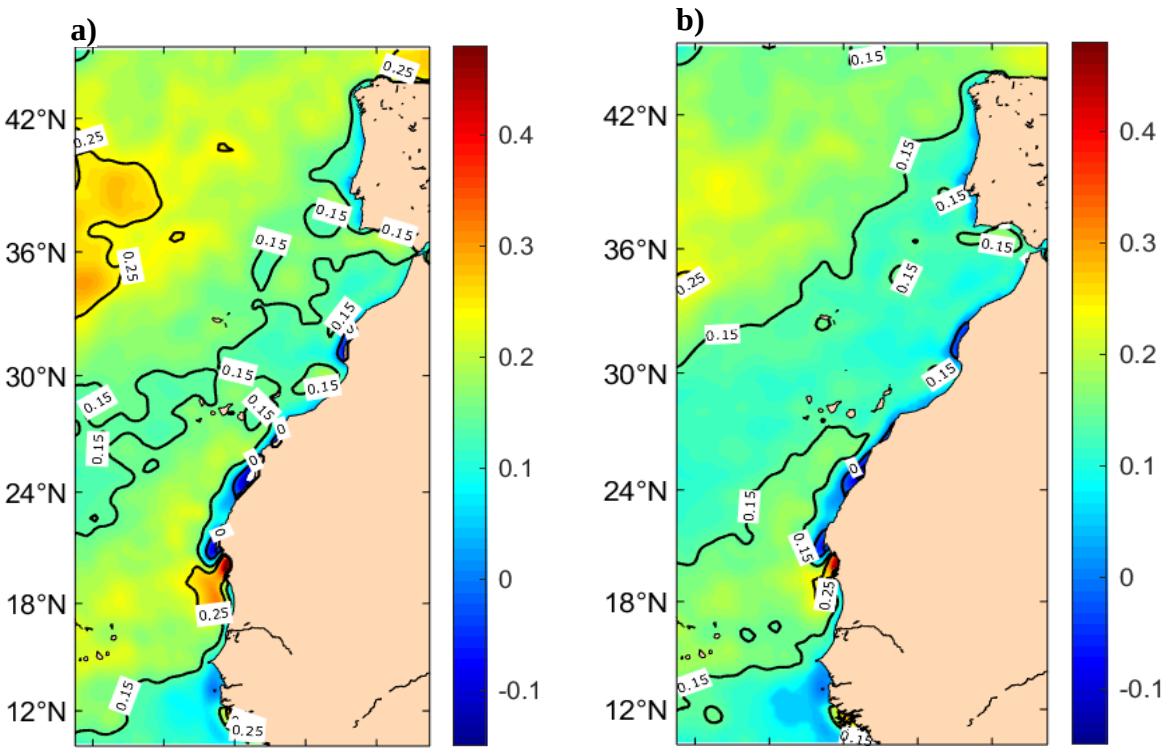

Figure 10: The map shows the trends of the CCMLE region with the color scale at left margin. **a)** correspond to the trends calculated from the uncorrected SST and **b)** represents the trends calculated from the corrected SST.

After the application of the transference function the trends smooth, however the negative and positive cells are preserved. A general smoother occurs in the open ocean as well. This might be due to a reduction of mesoscale process effects like upwelling filaments and eddies. But the structure of figure 11a is preserved after corrections.

5. DISCUSSION.

The presents results illustrate a comparison between *in-situ* and satellite-derived SST trends. The results of the comparison between the AVHRR/NOAA and the "Puertos del Estado" buoys (figure 5) indicate an overall good agreement between the *in-situ* observations and the satellite data, with the trends, with their confident intervals, not statistically discernible. Two of the buoys records area shorter than 30 years, and as indicated by Barton et al, (2013), the obtained trends could not reflect the climatic trend. Specifically, for the shorter records from the SC and PE buoys (REDCOS network), the drop in SST during the last years of the record might be an important factor for the high

significative trends. For the GC buoy, the use of deseasonalized data determined the reduction of the confident intervals.

For the EN4, that also include *in-situ* data, the results (figure 5b) indicate statistical significate differences with the AVHRR/NOAA, than are reduced after 2005, in correlation with the increase of the Argo floats which provide sustainability to the interpolation of the data. For that reason, the trends observed with the EN4 dataset do not match those observed with the AVHRR/NOAA. Nevertheless, AVHRR/NOAA datasets in oceanic waters presents a great likeness with the other *in-situ* observations and the trends are (within the limits of the confident interval) the same. On the other hand, in the comparative with the buoys there is also a good agreement with the MODIS dataset. The trends of this record coincide with several buoys' trends.

The previous comparison was done in open ocean waters, however, satellite products have more uncertainty close to the coast, due to the presence of clouds. As a difficulty added to this problem, the lack of long and stable measurements near the coast upwelling made harder the analysis of the influence of this interference. We use the RaProCan data set to approach this problem. The results (table 4 and figure 7) support the increase the satellite uncertainty as we approximate to the coast. But it is important to understand the limitation of this analysis: It has fewer measures compare to the rest datasets, so the uncertainty expected is greater, and as we had mentioned upwelling subsection is a proxy to the area because there is not data as near as it will be desirable. Nevertheless, this is a good orientate analysis that support the need to constitute long records near the upwelling area.

The correlations between *in-situ* and satellite data show significantly differences in the areas of the study. This supports the use of two different transfer equation for each area. Figure 9 show the selected coordinates to study the effects of these equations. For the open ocean area, the transference function eliminates a variability around the 20%. And, for the upwelling area, the variability reduction increase to 40%. This is exemplified in figure 10 applying the equation to two different open ocean areas (figure 10a and 10b) and two upwelling centers (figure 10c and 10d). Figures 10c correspond to a not statistically significative trend (see table 4). The results of Arístegui et al, (2009) reveal the seasonal pattern of this upwelling center. This could be an explanation to the greater uncertainty of the trend in UP1 (figure 10c) than in UP2 (figure 10d) which is a permanent upwelling (according to Arístegui et al, 2009). The present results of figure 10c and 10d support the needs of seasonal analyses to forecast properly the future of the upwelling.

The validation of the satellite derived-SST observations *in*-situ is one of the objectives of this work. Thus, as not variation in the pattern of the trends of figure 11 after corrections were detected, the results support the validate of the AVHRR/NOAA SST long-term

analyses derived from remote sensing. Once the reliability of the satellite data is accepted, we can discuss the changes in the CCMLE upwelling processes that offer the results. The hypothesis of an intensification of the upwelling process due to climate change propose by Bakun (1990) has been widely discuss as we commented in section 1. Global studies like Belkin (2009) of all the LME might be not representative due to the seasonal pattern and the spatial distribution of the upwelling centers. So, for example the warming trend in the average of all the CCMLE region presented by Belkin (2009) is not representative of the trend in the upwelling cells shown in figure 11 (both uncorrected and corrected). Regional studies like McGregor et al (2007) in the Cape Ghir (UP1 area in this study) support the hypothesis of Bakun (1990) but obtained significative trends, Barton et al (2013) reply arguing that the proxy based on alkenone unsaturation index ($U_{37}^{K'}$) extracted from coccolithophorids used by McGregor et al (2007) underestimate the SST and expose warming trends in the area. Nevertheless, Barton et al (2013) ignore the seasonality of the upwelling center describe by Arístegui et al (2009) so, as discussed before, seasonal analyses are required to obtained definitive results.

The negative trends in the upwelling center and the positively marked trend center around 18º N that correspond to downwelling process (which shared origins cause with the upwelling) presented in figure 11 are consistent with the Bakun's hypothesis (Bakun, 1990). However, the changes observed in the SST are not reflected in recent winds stress studies (Barton et al, 2013 and (Marrero-Betancort et al., 2020), since these authors found a net decrease of the winds trade intensity. Nonetheless, the wind stress field have complicated relation with upwelling process and the intensity is not only important variable but the combination of the wind direction and intensity. The work of Marrero-Betancort et al (2020) report a net trend to rotate clockwise the wind direction of 10.7º. Hence, both variable needs to combine when tried to forecast the evolution of the upwelling through the wind stress.

6. CONCLUSION

The results of long-term trends analyses of available SST records both *in-situ* and from remote sensing carried out in this study can be summarized as follows:

- The *in-situ* and satellite-derived AVHRR/NOAA SST agreement is supported both by the convergence of their trends and the high correlation through the OLS linear regression.
- The RaProCan subsections support the difference in the correlations of *in-situ* and satellite data between the open ocean area and the coast upwelling area due to coast interference.

- Although this sensibility lower on the satellite measures near the coast, the satellite observations keep the spatial pattern of the trends in the CCMLE region.
- The observed decrease in the temperature of the upwelling centers in this work support the hypothesis of an intensification upwelling intensity due to climate change, as suggested by Bakun (1990)

7. BIBLIOGRAPHY.

Alma, Ö. G. (2011). Comparison of Robust Regression Methods in Linear Regression. *Int. J. Contemp. Math. Sciences*, *6*(9), 409–421. http://m-hikari.com/ijcms-2011/9-12-2011/almaIJCMS9-12-2011.pdf

Arístegui, J., Barton, E. D., Álvarez-Salgado, X. A., Santos, A. M. P., Figueiras, F. G., Kifani, S., Hernández-León, S., Mason, E., Machú, E., & Demarcq, H. (2009). Sub-regional ecosystem variability in the Canary Current upwelling. *Progress in Oceanography*, *83*(1–4), 33–48. https://doi.org/10.1016/j.pocean.2009.07.031

Bakun, A. (1990). Coastal Ocean Upwelling. *Science*, *247*(4939), 198–201. https://doi.org/10.1126/science.247.4939.198

Barton, E. D., Field, D. B., & Roy, C. (2013). Canary current upwelling: More or less? *Progress in Oceanography*, *116*, 167–178. https://doi.org/10.1016/j.pocean.2013.07.007

Beaton, A. E., & Tukey, J. W. (1974). The Fitting of Power Series, Meaning Polynomials, Illustrated on Band-Spectroscopic Data. *Technometrics*. https://doi.org/10.1080/00401706.1974.10489171

Belkin, I. M. (2009). Rapid warming of Large Marine Ecosystems. *Progress in Oceanography*, *81*(1–4), 207–213. https://doi.org/10.1016/j.pocean.2009.04.011

Cracknell, A. P. (1996). The advanced very high resolution radiometer (AVHRR). In *The advanced very high resolution radiometer (AVHRR)*.

Donlon, C. J., Martin, M., Stark, J., Roberts-Jones, J., Fiedler, E., & Wimmer, W. (2012). The Operational Sea Surface Temperature and Sea Ice Analysis (OSTIA) system. *Remote Sensing of Environment*. https://doi.org/10.1016/j.rse.2010.10.017

Ekman, V. W. (1905). On the Influence of the Earth's Rotation on Ocean-Currents. In *Ark. Mat. Astr. Fys.* (Vol. 2, Issue 11). Almqvist & Wiksells. http://www.aos.princeton.edu/WWWPUBLIC/gkv/history/general.html

Eugenio, F., Marcello, J., Hernández-Guerra, A., & Rovaris, E. (2005). Regional optimization of an atmospheric correction algorithm for the retrieval of sea surface temperature from the Canary Islands-Azores Gibraltar area using NOAA/AVHRR data. *International Journal of Remote Sensing*, *26*(9), 1799–1814. https://doi.org/10.1080/01431160582000298341

Good, S. A., Martin, M. J., & Rayner, N. A. (2013). EN4: Quality controlled ocean temperature and salinity profiles and monthly objective analyses with uncertainty estimates. *Journal of Geophysical Research: Oceans*, *118*(12), 6704–6716. https://doi.org/10.1002/2013JC009067

Kämpf, J., & Chapman, P. (2016). Upwelling Systems of the World. In *Upwelling*

Systems of the World. https://doi.org/10.1007/978-3-319-42524-5

Legeckis, R. (1975). Application of synchronous meteorological satellite data to the study of time dependent sea surface temperature changes along the boundary of the Gulf Stream. *Geophysical Research Letters*. https://doi.org/10.1029/GL002i010p00435

Marrero-Betancort, N., Marcello, J., Rodríguez Esparragón, D., & Hernández-León, S. (2020). Wind variability in the Canary Current during the last 70 years. *Ocean Science*, *16*(4), 951–963. https://doi.org/10.5194/os-16-951-2020

McClain, E. P., Pichel, W. G., & Walton, C. C. (1985). Comparative performance of AVHRR-based multichannel sea surface temperatures. *Journal of Geophysical Research*. https://doi.org/10.1029/jc090ic06p11587

McGregor, H. V., Dima, M., Fischer, H. W., & Mulitza, S. (2007). Rapid 20th-Century Increase in Coastal Upwelling off Northwest Africa. *Science*, *315*(5812), 637–639. https://doi.org/10.1126/science.1134839

Merchant, C. J., Embury, O., Rayner, N. A., Berry, D. I., Corlett, G. K., Lean, K., Veal, K. L., Kent, E. C., Llewellyn-Jones, D. T., Remedios, J. J., & Saunders, R. (2012). A 20year independent record of sea surface temperature for climate from Along-Track Scanning Radiometers. *Journal of Geophysical Research: Oceans*. https://doi.org/10.1029/2012JC008400

Minnett, P. J., Alvera-Azcárate, A., Chin, T. M., Corlett, G. K., Gentemann, C. L., Karagali, I., Li, X., Marsouin, A., Marullo, S., Maturi, E., Santoleri, R., Saux Picart, S., Steele, M., & Vazquez-Cuervo, J. (2019). Half a century of satellite remote sensing of sea-surface temperature. *Remote Sensing of Environment*, *233*(August). https://doi.org/10.1016/j.rse.2019.111366

Mudelsee, M. (2019). Trend analysis of climate time series: A review of methods. *Earth-Science Reviews*, *190*(October 2018), 310–322. https://doi.org/10.1016/j.earscirev.2018.12.005

Narayan, N., Paul, A., Mulitza, S., & Schulz, M. (2010). Trends in coastal upwelling intensity during the late 20th century. *Ocean Science*. https://doi.org/10.5194/os-6-815-2010

Pauly, D., & Christensen, V. (1995). Primary production required to sustain global fisheries. *Nature*, *376*(6537), 279–279. https://doi.org/10.1038/376279b0

Rayner, N. A., Brohan, P., Parker, D. E., Folland, C. K., Kennedy, J. J., Vanicek, M., Ansell, T. J., & Tett, S. F. B. (2006). Improved analyses of changes and uncertainties in sea surface temperature measured in Situ since the mid-nineteenth century: The HadSST2 dataset. *Journal of Climate*. https://doi.org/10.1175/JCLI3637.1

Reynolds, R. W., Smith, T. M., Liu, C., Chelton, D. B., Casey, K. S., & Schlax, M. G. (2007). Daily high-resolution-blended analyses for sea surface temperature. *Journal of Climate*, *20*(22), 5473–5496. https://doi.org/10.1175/2007JCLI1824.1

Sherman, K., & Hempel, G. (2008). The UNEP Large Marine Ecosystem Report: A perspective on changing conditions in LMEs of the world's Regional Seas. In *UNEP Regional Seas Reports and Studies* .

Vélez-Belchí, P, Hernández-Guerra, A., Barrera, C., Fraile-Nuez, E., Barrera, A., LLinas, O., Benítez-Barrios, V. M. (Verónica M., Domínguez, F., Alonso-González, I.,

González Dávila, M., Santana Casiano, M., Hernández Brito, J. J., Presas-Navarro, C., Arístegui Ruiz, J., Comas-Rodriguez, I., Garijo Lopez, J. C., Hernández León, S., Pérez-Hernández, M. D., Rodríguez Santana, A., & Sosa-Trejo, D. (2014). *Monitoring the Oceanic Waters of the Canary Islands: the deep hydrographic section of the Canaries*.

Vélez-Belchí, Pedro, Pérez-Hernández, M. D., Casanova-Masjoan, M., Cana, L., & Hernández-Guerra, A. (2017). On the seasonal variability of the Canary Current and the Atlantic Meridional Overturning Circulation. *Journal of Geophysical Research: Oceans*, *122*(6), 4518–4538. https://doi.org/10.1002/2017JC012774

Woodruff, S. D., Diaz, H. F., Kent, E. C., Reynolds, R. W., & Worley, S. J. (2008). The evolving SST record from ICOADS. In *Advances in Global Change Research*. https://doi.org/10.1007/978-1-4020-6766-2_4

Wooster, W. S., Bakun, a., & McLain, D. R. (1976). The seasonal upwelling cycle along the North Atlantic. *Journal of Marine Research*.